

The Upregulation of $\alpha_2\delta$ -1 Subunit Modulates Activity-Dependent Ca^{2+} Signals in Sensory Neurons

Marianna D'Arco, Wojciech Margas, John S. Cassidy, and Annette C. Dolphin

Department of Neuroscience, Physiology and Pharmacology, University College London, London WC1E 6BT, United Kingdom

As auxiliary subunits of voltage-gated Ca^{2+} channels, the $\alpha_2\delta$ proteins modulate membrane trafficking of the channels and their localization to specific presynaptic sites. Following nerve injury, upregulation of the $\alpha_2\delta$ -1 subunit in sensory dorsal root ganglion neurons contributes to the generation of chronic pain states; however, very little is known about the underlying molecular mechanisms. Here we show that the increased expression of $\alpha_2\delta$ -1 in rat sensory neurons leads to prolonged Ca^{2+} responses evoked by membrane depolarization. This mechanism is coupled to $\text{Ca}_v2.2$ channel-mediated responses, as it is blocked by a ω -conotoxin GVIA application. Once initiated, the prolonged Ca^{2+} transients are not dependent on extracellular Ca^{2+} and do not require Ca^{2+} release from the endoplasmic reticulum. The selective inhibition of mitochondrial Ca^{2+} uptake demonstrates that $\alpha_2\delta$ -1-mediated prolonged Ca^{2+} signals are buffered by mitochondria, preferentially activated by Ca^{2+} influx through $\text{Ca}_v2.2$ channels. Thus, by controlling channel abundance at the plasma membrane, the $\alpha_2\delta$ -1 subunit has a major impact on the organization of depolarization-induced intracellular Ca^{2+} signaling in dorsal root ganglion neurons.

Introduction

Calcium-activated signaling pathways underlie multiple cellular processes operating through complex spatial structures and a wide time range (Berridge et al., 2003). A tight balance between extracellular and intracellular calcium sources contributes to calcium dynamics in neurons where voltage-gated calcium channels (VGCCs) constitute the main regulators of calcium entry in response to membrane depolarization (Berridge, 1998). VGCCs are characterized by a pore-forming α 1 subunit associated with two accessory proteins, a cytosolic β subunit, and a membrane-anchored $\alpha_2\delta$ subunit (Bauer et al., 2010). $\alpha_2\delta$ subunits modulate calcium channel current kinetics and also increase trafficking of the channel to the plasma membrane (Dolphin, 2012; Cassidy et al., 2014). Recent findings indicate that $\alpha_2\delta$ proteins are crucial determinants of VGCC abundance at presynaptic terminals (Hoppa et al., 2012); thus, the overexpression of this subunit in hippocampal neurons promoted calcium channel localization at active zones, leading to an increase in vesicular release.

In sensory neurons, $\alpha_2\delta$ -1 function has been associated with mechanisms for generation and maintenance of chronic pain.

Peripheral nerve injury models of neuropathic pain in rodents resulted in a significant upregulation of $\alpha_2\delta$ -1 protein levels in cell bodies and axon terminals of dorsal root ganglion (DRG) neurons, with a consequent accumulation of presynaptic $\alpha_2\delta$ -1 protein in the dorsal horn of the spinal cord (Bauer et al., 2009). Conversely, damaged DRGs displayed no change in $\text{Ca}_v2.2$ mRNA or protein, which is the main VGCC type in sensory neurons (Xiao et al., 2002; Li et al., 2006). Although still debated, it is likely that the increased expression of $\alpha_2\delta$ -1 subunit induced by nerve injury may increase VGCC trafficking toward the cell surface and presynaptic terminals. In-line with this hypothesis, experiments performed in transgenic mice overexpressing $\alpha_2\delta$ -1 showed enhanced calcium currents recorded in DRG neurons, as well as nociceptive behavior characterized by hyperalgesia (Li et al., 2006). By contrast $\alpha_2\delta$ -1 knock-out mice had reduced DRG calcium currents and lower baseline mechanical sensitivity (Patel et al., 2013).

DRG neurons exhibit diverse patterns for the regulation of intracellular calcium (Lu et al., 2006), among which the endoplasmic reticulum (ER) and mitochondria are the main contributors to activity-induced calcium increase (FERNYHOUGH and CALCUTT, 2010). The ER amplifies Ca^{2+} influx triggered by mild depolarization and promotes the propagation of a signal to the nucleus (Usachev and Thayer, 1997; Berridge, 1998), whereas mitochondria buffer high Ca^{2+} loads (Colegrove et al., 2000) particularly at synaptic terminals (Medvedeva et al., 2008). In this study, we show that the $\alpha_2\delta$ -1 subunit has a key role in regulating the handling of intracellular calcium in sensory neurons. The overexpression of $\alpha_2\delta$ -1 induces an upregulation of surface VGCCs and prolongs intracellular Ca^{2+} signals evoked by depolarization. Using pharmacological and genetic tools, we demonstrate that these sustained responses are mediated by augmented mitochondrial Ca^{2+} buffering of cytoplasmic Ca^{2+} increase induced by N-type channels.

Received Sept. 26, 2014; revised Feb. 4, 2015; accepted Feb. 5, 2015.

Author contributions: M.D. and A.C.D. designed research; M.D. and W.M. performed research; J.S.C. contributed unpublished reagents/analytic tools; M.D. and W.M. analyzed data; M.D. and A.C.D. wrote the paper.

This work was supported in part by a Newton Fellowship from the Royal Society to M.D., a Wellcome Trust senior Investigator award to A.C.D. (098360/Z/12/Z), and Medical Research Council (UK) Grants G0801756 and G0901758 to A.C.D., J.S.C. was supported by an MRC CASE PhD studentship with Pfizer. We thank Prof. Renato Rizzuto and Dr Anna Raffaello for providing wild-type and mutant MCU plasmids, Prof. Josef Kittler for mtdsred2 cDNA, and Dr Marianthi Papakosta for support in the initial development of HA- $\text{Ca}_v2.2$.

The authors declare no competing financial interests.

This article is freely available online through the *JNeurosci* Author Open Choice option.

Correspondence should be addressed to either Dr Marianna D'Arco or Prof. Annette Dolphin, Department of Neuroscience, Physiology and Pharmacology, University College London, Gower Street, London WC1E 6BT, UK. E-mail: m.d'arco@ucl.ac.uk or a.dolphin@ucl.ac.uk.

DOI:10.1523/JNEUROSCI.3997-14.2015

Copyright © 2015 the authors 0270-6474/15/355891-13\$15.00/0

Materials and Methods

DNA constructs. The cDNAs used in this study were as follows: $\alpha_2\delta$ -1 HA (Kadurin et al., 2012) $\alpha_2\delta$ -1 MIDAS^{AAA} HA (Hoppa et al., 2012), HA Ca_v2.2 (Cassidy et al., 2014), and ratiometric Pericam (Nagai et al., 2001) expressed in pcDNA3.0; pEYFP, pECFP and pdsRed2-Mito (Clontech), pcDNA3.1 MCU^{D260N,E263Q}-FLAG and MCU-FLAG (Raffaello et al., 2013), pRK5 β 1b, and Kir2.1-AAA (Tinker et al., 1996).

Reagents. Fura-2AM was purchased from Invitrogen, ω -conotoxin GVIA from Alomone. Nifedipine, cyclopiazonic acid (CPA), antimycin, and oligomycin were obtained from Sigma-Aldrich.

Neuronal culture and transfection. DRGs were isolated from P10 Sprague-Dawley rats of either sex. DRGs were dissociated in Hank's basal salt solution containing 5 mg/ml dispase (Invitrogen), 2 mg/ml collagenase (Worthington Biochemical), and 0.1 mg/ml DNase (Invitrogen) at 37°C for 30 min in a shaking water bath. Neuronal suspension was transfected by nucleofection following the manufacturer's instructions (Program G-13, Lonza). To improve cell viability after transfection, neurons were incubated in RPMI medium (Invitrogen) supplemented with 10% FBS (fetal bovine serum) and NGF (nerve growth factor; 50 ng/ml, Invitrogen) for 8 min at 37°C. DRGs were then plated on poly-L-lysine-coated coverslips (0.25 mg/ml, Sigma-Aldrich) and cultured in DMEM-F12 (Invitrogen) containing 10% FBS and 50 ng/ml NGF. $\alpha_2\delta$ -1 HA cDNA was cotransfected with eCFP or eYFP in a 4:1 ratio (2 μ g of total DNA). For the coexpression of $\alpha_2\delta$ -1 HA, MCU^{D260N,E263Q}-FLAG, and eYFP cDNAs, the ratio used was 4:3:1. In control conditions, $\alpha_2\delta$ -1 HA cDNA was replaced with an equivalent volume of empty vector. In live labeling experiments, control neurons were transfected with a control cDNA (Kir2.1-AAA cDNA encoding a nonfunctional potassium channel).

Calcium imaging. Calcium imaging was performed on somata of small (≤ 25 μ m) and medium (26–35 μ m) DRGs, 40 h after transfection. Neurons were loaded with Fura-2-AM or Fura-FF-AM in DMEM-F12 medium supplemented with 2% FBS for 20 min at 37°C and washed for 5 min with bathing solution containing the following (in mM): 145 NaCl, 5 KCl, 2 CaCl₂, 1 MgSO₄, 10 HEPES, 10 Glucose, pH 7.4 and placed in a recording chamber under continuous superfusion (flow rate of 2.5–3 ml/min). Ca^{2+} -free experiments were performed using a solution corresponding to the normal extracellular solution modified by the omission of CaCl₂, the addition of 0.1 mM EGTA and 2 mM MgCl₂ (Lu et al., 2006). Fura-2 and Fura-FF-loaded neurons were visualized on 20 \times objective with a Zeiss Axiovert 200M inverted microscope. Data were acquired using two imaging systems: Improvion Volocity software connected to a CCD camera (ORCA-ER; Hamamatsu Photonics) or MetaFluor Fluorescence Ratio Imaging Software (Cairn Research) via an iXon Ultra 897 camera (Andor Technology). Fura-2 excitation wavelengths at 340 and 380 nm were controlled either by a filter wheel or via an Optoscan monochromator (Cairn Research). Dual excitation filter at 340 and 380 nm, 400 nm dichroic mirror, and emission at 510/80 nm were purchased from Chroma Technology. Ratio signals were sampled at 0.5–1 Hz. Fluorescence was quantified within a region-of-interest after background subtraction. After confirmation of a stable baseline, neurons were depolarized by high K⁺ (50 or 100 mM, 10 s) or field stimulation (10 or 100 Hz). A positive response was defined as a 50% fluorescence increase with respect to the baseline. Only one field of neurons was recorded from each coverslip. No difference in the percentage of responding neurons was detected between control ($41.5 \pm 6.1\%$, total $n = 86$) and $\alpha_2\delta$ -1 neurons ($48.7 \pm 5.8\%$, total $n = 96$; $p = 0.4$, t test). Peak amplitude was measured as the maximal signal observed within 20 s after depolarization, whereas the duration of a response was determined as the width at 25% of the maximal signal. For measurement of mitochondrial Ca^{2+} , DRG neurons were transfected with ratiometric mtPericam (Nagai et al., 2001) and visualized on a 40 \times oil-immersion objective. The mitochondrial Ca^{2+} probe was excited at the pH insensitive wavelength of 380 nm using the Fura-2 excitation filter as described previously (Akimzhanov and Boehning, 2011). [Ca^{2+}]_{mt} was measured as $-(F - F_0)/F_0$ (Shutov et al., 2013) where F is the fluorescence at 380 nm and F_0 is the baseline fluorescence acquired before stimulation. Images were acquired at 1 Hz. Positively transfected neurons were identified by eYFP

or mcherry fluorescence in Fura-2 or mtPericam imaging experiments respectively.

Neuron replating. To remove neurite outgrowths and improve control of membrane potential in voltage-clamp experiments, neurons were replated as previously described (Page et al., 2010). Briefly, cells were incubated in a collagenase solution (0.2 mg/ml in serum free DMEM-F12) at 37°C for 10 min. Neurons were then resuspended in DMEM-F12/FBS and plated on poly-L-lysine-coated coverslips. Voltage-clamp experiments were performed 2–6 h after replating.

Electrophysiology. As for calcium imaging, whole-cell voltage-clamp experiments were performed in small (< 19 pF) and medium (20–38 pF) DRG neurons. Recordings were performed with Axopatch 200A amplifier (Molecular Devices) and analyzed with pClamp 9.0 software (Molecular Devices). Whole-cell voltage-clamp recordings were sampled at 10 kHz frequency, filtered at 2 kHz and digitized at 1 kHz. 80–85% series resistance compensation was applied and all recorded currents were leak subtracted using P/4 protocol. The extracellular solution for recording Ba²⁺ currents contained the following (in mM): 10 BaCl₂, 150 TEABr, 3 KCl, 1 NaHCO₃, 1 MgCl₂, 10 HEPES, 4 glucose, 0.001 TTX, pH 7.4, 320 mOsm. The patch internal solution contained the following (in mM): 140 Cs aspartate, 5 EGTA, 2 MgCl₂, 0.1 CaCl₂, 2 K₂ATP, 10 HEPES, pH 7.2, 292 mOsm. Membrane potential was held at -90 mV. For current-clamp experiments, the following solutions were used: extracellular (in mM): 145 NaCl, 5 KCl, 2 CaCl₂, 1 MgSO₄, 10 HEPES, and 10 glucose, pH 7.4, 316 mOsm; internal (in mM): 130 KCl, 10 EGTA, 10 HEPES, 8 NaCl, 4 Mg-ATP, 1 MgCl₂, 1 CaCl₂, 0.4 Na₂-GTP, pH 7.25 adjusted with 1 M KOH, 318 mOsm. Recording pipettes had access resistance of 1–4 M Ω . For recordings performed in the presence of CTX, the drug was superfused for 100 s at 1 μ M concentration. Currents were measured before and after drug application at 6 ms after the start of a 15 mV test pulse.

Immunocytochemistry. For live labeling experiments DRG cultures were incubated with a monoclonal anti-HA antibody (rat, 1:250; Roche) for 1 h at 37°C in bathing solution. This procedure, followed by cell fixation and application of a secondary antibody in nonpermeabilizing conditions, allowed the labeling of plasma membrane $\alpha_2\delta$ -1 HA subunits without contamination from intracellular proteins. Briefly, after primary antibody incubation neurons were fixed with 4% PFA in PBS for 5 min and then blocked for 30–60 min with PBS supplemented with 10% goat serum. AlexaFluor-conjugated secondary antibody (1:500, Invitrogen) was incubated for 1 h at RT. For detection of intracellular proteins following surface labeling, neurons were permeabilized with 0.1% Triton for 8 min and then incubated with a primary antibody (1 h at RT). Samples were mounted on slides using Vectashield (Vector Laboratories) to reduce photobleaching. Imaging was performed using a confocal laser-scanning microscope (Zeiss) and a 40 \times oil-immersion objective. Optical sections of 1 μ m thickness were acquired for each channel.

The approximate transfection efficiency of the $\alpha_2\delta$ -1 HA subunit in DRG neurons was quantified by staining with an antibody against the HA epitope to be 32%, ($n = 124$ cells examined); this corresponded to an $\alpha_2\delta$ -1 expression increase of $160 \pm 30\%$ ($n = 139$) compared with control endogenous proteins labeled with $\alpha_2\delta$ -1 antibody ($n = 142$).

For quantitative analysis of neurite outgrowth patterns, live-labeled neurons were scored with respect to neurite length (average length of two longest neurites) and branching (average number of neuritic branch points per neurite length). The analysis was performed using NeuronJ software (Meijering et al., 2004).

Mitochondrial time lapse imaging. Neurons were transfected with eCFP, pdsRed2-Mito, $\alpha_2\delta$ -1 HA, or $\alpha_2\delta$ -1MIDAS^{AAA} HA cDNAs in a 1:1:4 ratio. Forty hours after transfection, cultures were imaged at 37°C in bathing solution. Images were acquired every 2 s for 10 min. The percentage of moving mitochondria was analyzed in the distal part of neurites (100–150 μ m from the soma). Before electrical stimulation (100 Hz, 10 s) neurons were imaged for 3 min in resting conditions. Mitochondria were defined as moving if they moved > 1 μ m in 1 min. Kymograph analysis was performed using ImageJ software as previously described (Macaskill et al., 2009). Kymographs were generated from live-imaging movies of 3 min before and after field stimulation. Moving mitochondria were identified using Manual Tracker plugin from ImageJ.

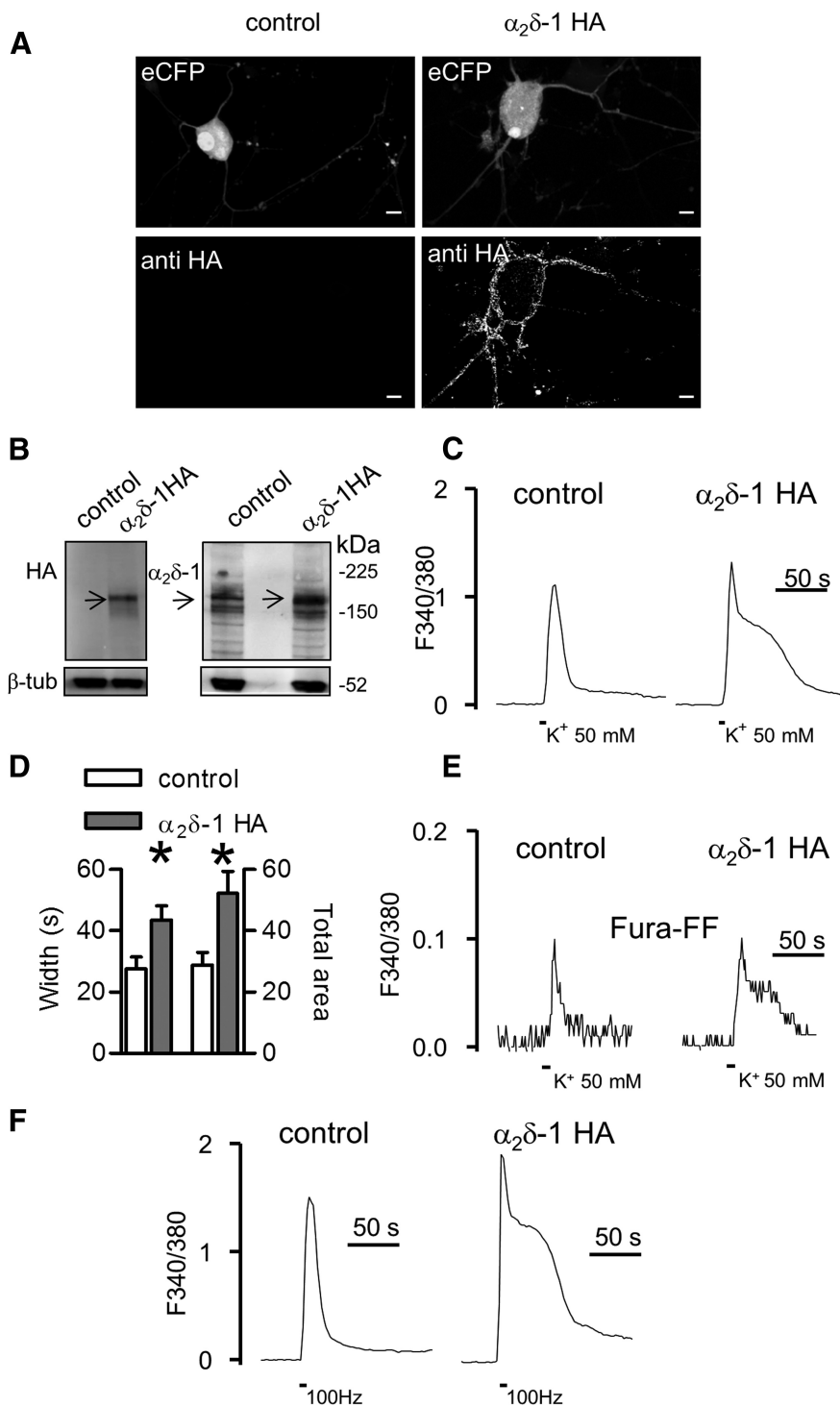


Figure 1. $\alpha_2\delta$ -1 HA overexpression modulates Ca^{2+} response duration in DRG neuron cultures. **A**, 3D projection from z-stacks of confocal images of a DRG neuron transfected with $\alpha_2\delta$ -1 HA and eCFP (right) or eCFP and nonfunctional Kir2.1-AAA cDNAs (left). Exogenous $\alpha_2\delta$ -1 HA proteins were detected at the cell surface by live labeling ($n = 6$ experiments). No staining for the HA epitope was observed in neurons expressing eCFP only. Scale bars, 10 μ m. **B**, Western blotting of neuronal lysates of eCFP or $\alpha_2\delta$ -1 HA transfected DRGs. Lysates were loaded in duplicate and the membrane was probed for HA (left) or $\alpha_2\delta$ -1 subunit expression. The neuronal content was quantified by β tubulin III (β -tub) staining ($n = 8$ DRG cultures, 4 gels). **C**, Fura-2 imaging of high K^+ -evoked Ca^{2+} transients performed in control (left; representative of $n = 19$) and $\alpha_2\delta$ -1 HA overexpressing neurons (right; representative of $n = 24$). Traces are shown after baseline subtraction. **D**, Control, open bars; $\alpha_2\delta$ -1 HA, gray bars. The width and total area of transients were significantly higher in $\alpha_2\delta$ -1 HA overexpressing neurons with respect to control DRGs ($*p = 0.01$, t test). **E**, Representative Fura-FF transients imaged in control ($n = 11$) and $\alpha_2\delta$ -1 HA neurons ($n = 7$). **F**, Examples of Ca^{2+} transients induced by field stimulation (100 Hz, 10 s) of control (left) and $\alpha_2\delta$ -1 HA DRGs (right).

Western blotting. DRG cultures transfected with eCFP (2 μ g) or $\alpha_2\delta$ -1 HA (2 μ g) cDNAs were harvested in buffer A (50 mM Tris, pH7.5, 50 mM NaCl, and protease inhibitors; Complete, Roche). Neuronal suspensions were centrifuged at $60,000 \times g$ for 1 h at 4°C. Pellets were lysed for 40 min at 4°C in buffer A supplemented with 1% Igepal and then centrifuged at $14,000 \times g$ for 30 min at 4°C. Lysates were resolved by SDS-Page (3–8% NuPage Tris/acetate gels, Invitrogen), transferred to PVDF membranes and probed with antibodies to $\alpha_2\delta$ -1 (mouse, 1:2000; Sigma-Aldrich) and β -tubulin III (rabbit, 1:2000; Sigma-Aldrich). Optical density quantification was performed with ImageJ. In every sample, the $\alpha_2\delta$ -1 signal was normalized with respect to β -tubulin III content.

Statistical analysis. Data were analyzed with GraphPad Prism 4.0 software or Origin7 (OriginLab). All data are shown as mean \pm SEM; “ n ” refers to number of cells, unless indicated otherwise. The statistical significance between two groups was assessed by t test or Mann–Whitney U test. One-way ANOVA was used for comparison of means between three or more groups and two-way ANOVA to analyze the effect of two variables on an experimental response.

Results

Characterization of $\alpha_2\delta$ -1 HA overexpressing neurons

$\alpha_2\delta$ -1 Protein was overexpressed by nucleofection (Karra and Dahm, 2010) in DRG cultures obtained from postnatal rats. This *in vitro* model preserved most neuronal properties displayed by DRGs *in vivo* (Wood et al., 1988). To identify the expression of exogenous $\alpha_2\delta$ -1 protein we used a construct engineered with an extracellular HA tag throughout these studies ($\alpha_2\delta$ -1 HA; Kadurin et al., 2012). Exogenous $\alpha_2\delta$ -1 HA subunits were found to be well expressed and localized at the cell surface in DRG cell bodies and neurites visualized with free eCFP (Fig. 1A). Upon transfection, the total expression of $\alpha_2\delta$ -1 protein in neuronal lysates was increased by $63 \pm 27\%$ with respect to the control, as quantified by Western blotting (Fig. 1B, right; $p = 0.02$, Mann–Whitney U test). Overexpressed $\alpha_2\delta$ -1 protein was also identified by an HA antibody (Fig. 1B, left). To examine whether $\alpha_2\delta$ -1 transfection might affect neuronal morphology, we analyzed neurite outgrowth in control and $\alpha_2\delta$ -1 HA overexpressing neurons (see Materials and Methods). No difference in neurite length (control: $106.4 \pm 11.2 \mu$ m, $n = 8$; $\alpha_2\delta$ -1 HA: $108.2 \pm 15.7 \mu$ m, $n = 6$; $p = 0.92$, t test) or number of branch points (control: $0.013 \pm 0.004 \mu$ m $^{-1}$, $\alpha_2\delta$ -1 HA: $0.010 \pm 0.002 \mu$ m $^{-1}$; $p = 0.52$, t test) were measured between control and $\alpha_2\delta$ -1 overexpressing DRGs.

Table 1. Electrophysiological properties of control and $\alpha_2\delta$ -1 DRGs

Parameters	Control (<i>n</i> = 26)	$\alpha_2\delta$ -1 (<i>n</i> = 31)	<i>p</i> (<i>t</i> test)
V_{rest} (mV)	-58.9 ± 0.8	-56.7 ± 1.0	0.1
V_{K^+} (mV)	-18.4 ± 0.7	-17.7 ± 0.6	0.4
AP	4.5 (2, 8)	6.0 (4, 9)	0.9

V_{rest} , Resting membrane potential; V_{K^+} , membrane potential during 50 mM K^+ ; AP, median number of action potentials (25 and 75% percentile).

Next we addressed the impact of $\alpha_2\delta$ -1 HA overexpression on Ca^{2+} entry. DRGs are a heterogeneous population of neurons, where function correlates with cell size (Basbaum et al., 2009). For this reason we focused our functional studies on the two major classes of nociceptors corresponding to small (<25 μ m) and medium (25–35 μ m) diameter DRG neurons, which are known to give rise respectively to C and A δ afferent sensory fibers (Julius and Basbaum, 2001). We performed Fura-2 imaging on DRG cultures depolarized by a 10 s application of high (50 mM) K^+ . Table 1 summarizes some electrophysiological properties measured in current-clamp recordings before and during high K^+ application to transfected neurons. Figure 1C shows representative high K^+ -evoked Ca^{2+} transients imaged 40–48 h after transfection in control and $\alpha_2\delta$ -1 overexpressing DRG neurons. The peak of the response was unaltered by $\alpha_2\delta$ -1 HA overexpression (control_{F340/380}: 2.03 ± 0.12 , *n* = 19; $\alpha_2\delta$ -1 HA_{F340/380}: 2.37 ± 0.16 , *n* = 24; *p* = 0.13), although in these neurons the Ca^{2+} signals displayed a slower recovery after the peak, leading to a prolonged Ca^{2+} rise (“ Ca^{2+} hump”; Fig. 1C, right trace). There was a significant increase of both response width and total area (Fig. 1D) of high K^+ -evoked Ca^{2+} transients in $\alpha_2\delta$ -1 HA overexpressing DRGs compared with control neurons. As shown in Figure 1E, a slower recovery of the response in $\alpha_2\delta$ -1 HA overexpressing neurons was also observed in the presence of the lower affinity Ca^{2+} dye, Fura-FF.

A similar modulation of Ca^{2+} signals was observed when cultures were field-stimulated at 100 Hz for 10 s. As illustrated in Figure 1F, intense electrical stimulation induced an extended Ca^{2+} rise in neurons transfected with $\alpha_2\delta$ -1 HA (55 ± 7 s, *n* = 10), but not in the control neurons (32 ± 8 s, *n* = 7; *p* = 0.04, *t* test). By contrast, no change in response width was detected when neurons were stimulated at a lower (10 Hz) frequency (control: 37.6 ± 5.8 s, *n* = 18; $\alpha_2\delta$ -1 HA DRGs: 41.1 ± 4.3 s, *n* = 18; *p* = 0.63, *t* test), indicating that the $\alpha_2\delta$ -1-mediated Ca^{2+} hump depended on a sustained activation of VGCCs.

Mutation of the extracellular MIDAS motif prevents $\alpha_2\delta$ -1 HA effects on Ca^{2+} signals

$\alpha_2\delta$ Subunits are characterized by a conserved von Willebrand A domain (VWA), which mediates the interaction with extracellular proteins through the metal-ion-dependent adhesion site motif (MIDAS). This consensus sequence is involved in the coordination of divalent cations and has been found to be essential for the ability of $\alpha_2\delta$ -1 and $\alpha_2\delta$ -2 to modulate VGCC function (Cantí et al., 2005; Hoppa et al., 2012) and trafficking (Cassidy et al., 2014). We transfected DRG neurons with an $\alpha_2\delta$ -1 construct carrying three point mutations within the MIDAS motif ($\alpha_2\delta$ -1 MIDAS^{AAA} HA; Hoppa et al., 2012) and examined the effect of the mutant subunit overexpression on Ca^{2+} signaling. First we monitored $\alpha_2\delta$ -1 MIDAS^{AAA} HA protein expression in DRG cultures using a combined staining of the cell surface via live labeling, followed by detection of intracellular $\alpha_2\delta$ -1 HA after cell permeabilization (Fig. 2A). Figure 2B quantifies the ratio be-

tween surface and cytosolic HA staining in $\alpha_2\delta$ -1 HA and $\alpha_2\delta$ -1 MIDAS^{AAA} HA transfected neurons. There was a marked reduction of surface expression of $\alpha_2\delta$ -1 MIDAS^{AAA} compared with wild-type $\alpha_2\delta$ -1 whereas the expression of intracellular $\alpha_2\delta$ -1 was unchanged in the examined cells (intra $\alpha_2\delta$ -1 HA: 85.4 ± 15.1 A.U., *n* = 9; intra $\alpha_2\delta$ -1 MIDAS^{AAA} HA: 79.8 ± 19.7 A.U., *n* = 5; *p* = 0.82, *t* test).

In-line with previous findings (Cantí et al., 2005; Hoppa et al., 2012), patch-clamp experiments confirmed that $\alpha_2\delta$ -1 MIDAS^{AAA} was unable to potentiate Ca^{2+} current density, whereas the overexpression of wild-type $\alpha_2\delta$ -1 strongly increased current density (Fig. 2C,D). When we examined the impact of the MIDAS mutation on intracellular Ca^{2+} signals we found that overexpression of $\alpha_2\delta$ -1 MIDAS^{AAA} HA did not alter the shape of Ca^{2+} transients (Fig. 2E), producing responses with a duration similar to the control group and with faster recovery compared with wild-type $\alpha_2\delta$ -1 HA overexpressing neurons (Fig. 2F). These results suggest that the presence of a functional $\alpha_2\delta$ -1 subunit at the cell surface is critical for its regulatory role on neuronal Ca^{2+} pathways.

Role of $Ca_v2.2$ channels in $\alpha_2\delta$ -1 HA mediated prolongation of Ca^{2+} signals

DRG neurons express a number of different VGCC subtypes and $Ca_v2.2$ (N-type) channels represent the main contributors to membrane depolarization-induced calcium influx (Scroggs and Fox, 1992; Bell et al., 2004). To investigate the influence of the different VGCCs on Ca^{2+} responses shaped by $\alpha_2\delta$ -1 HA overexpression, we performed Fura-2 imaging in the presence of ω -conotoxin GVIA (CTX, 1 μ M) or nifedipine (Nif, 1 μ M), which are respectively N- and L-type (Ca_v1) channel blockers (Fig. 3A–F). As shown in Figure 3A,D, the peak amplitude of high K^+ -evoked Ca^{2+} transients of both control and $\alpha_2\delta$ -1 overexpressing neurons was reduced by 15 min pretreatment with CTX. Moreover in $\alpha_2\delta$ -1 HA overexpressing DRGs, the block of $Ca_v2.2$ channels abolished the prolongation of the Ca^{2+} signals (Fig. 3F). By contrast, in control neurons, CTX application had no effect on response width (Fig. 3C), suggesting that $Ca_v2.2$ channels are involved in $\alpha_2\delta$ -1 modulation of the Ca^{2+} increase. Also we observed that Ca_v1 family channels were not critical for the generation of responses evoked by 50 mM K^+ , because continuous superfusion of DRG cultures with nifedipine did not change the shape of the Ca^{2+} transient, either in control (Fig. 3B,C) or in $\alpha_2\delta$ -1 HA overexpressing neurons (Fig. 3E,F). Thus the contribution of $Ca_v2.2$ channels in response to a strong depolarization is much greater than the Ca_v1 channel contribution to intracellular Ca^{2+} signals in DRG somata, as previously described for sympathetic neurons (Wheeler et al., 2012).

In agreement with these results, in whole-cell patch-clamp recordings CTX application significantly reduced Ba^{2+} current density of control (-64 ± 8 pA/pF, *n* = 10) and $\alpha_2\delta$ -1 overexpressing neurons (-103 ± 19 pA/pF, *n* = 11) to -31 ± 5 pA/pF and -37 ± 7 pA/pF respectively (*p* < 0.01, *t* test), indicating a greater percentage of current blocked by CTX in the presence of $\alpha_2\delta$ -1 subunit ($63 \pm 2\%$) compared with control condition ($53 \pm 3\%$; *p* = 0.016, *t* test).

Next, to address the hypothesis that $\alpha_2\delta$ -1 overexpression could indeed modulate surface N-type calcium channels, neurons were cotransfected with $\alpha_2\delta$ -1 cDNA and a $Ca_v2.2$ construct containing an HA tag in an extracellular loop (Cassidy et al., 2014). This technique was used because the lack of commercially available antibodies directed against extracellular epitopes prevented the detection of native surface-expressed $Ca_v2.2$ subunits.

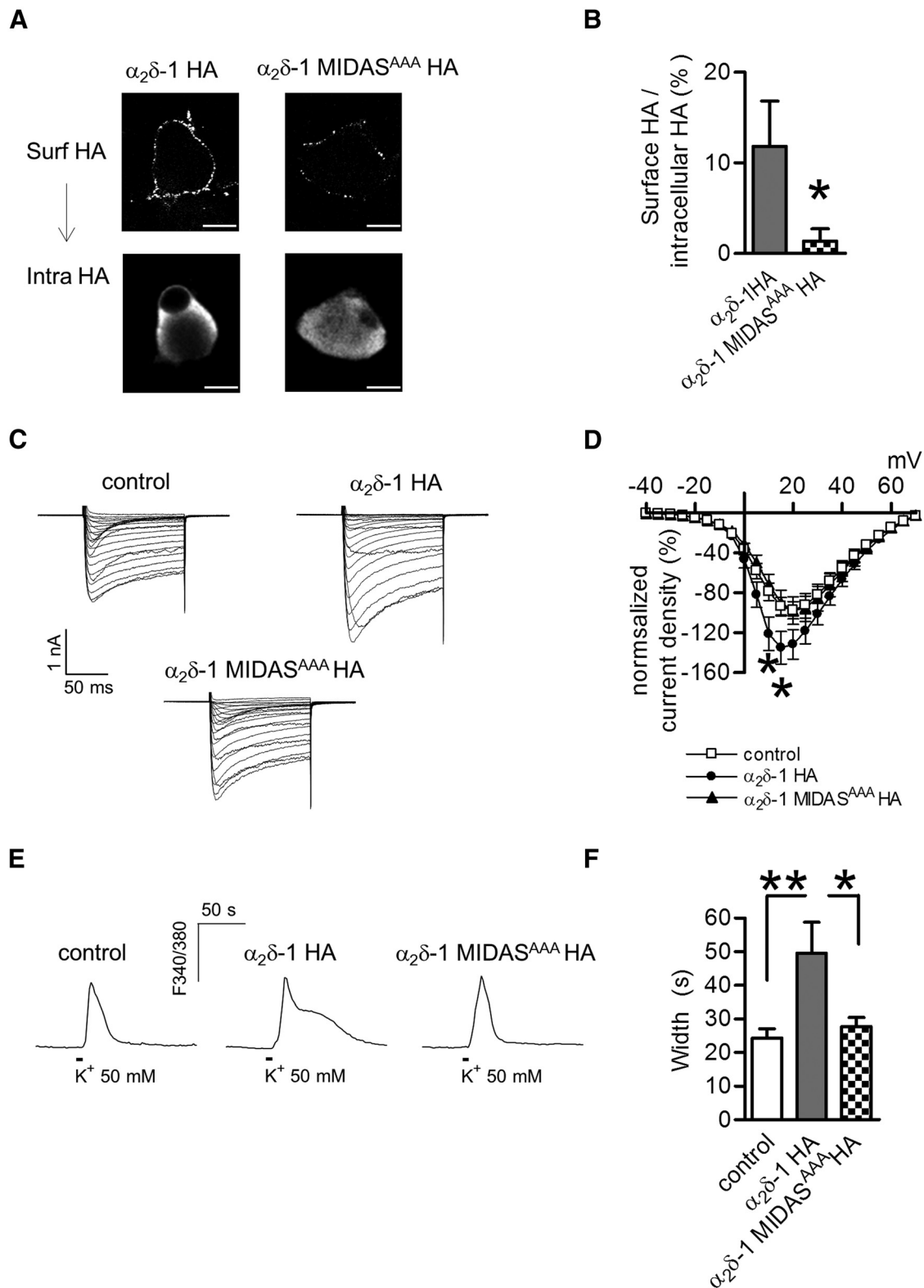


Figure 2. Expression of $\alpha_2\delta$ -1 MIDAS^{AAA} HA in DRG cultures. **A**, Confocal images of DRG neurons transfected with $\alpha_2\delta$ -1 HA or $\alpha_2\delta$ -1 MIDAS^{AAA} HA subunits. Top, Cell surface HA (Surf HA). Scale bar, 10 μ m. Positively transfected neurons were identified following detection of intracellular HA-tagged proteins (intra HA, bottom). **B**, Quantification of surface HA fluorescence for wild-type $\alpha_2\delta$ -1 HA overexpressing neurons (gray bar; $n = 9$) and $\alpha_2\delta$ -1 MIDAS^{AAA} HA (checked bar; $n = 5$). Membrane HA signal was normalized against the intracellular HA content ($*p = 0.01$, Mann–Whitney test). **C**, Examples of families of I_{Ca} current traces for control, $\alpha_2\delta$ -1 HA and $\alpha_2\delta$ -1 MIDAS^{AAA} HA overexpressing DRG neurons. Currents were evoked from -90 mV holding potential in 5 mV steps from -40 to $+70$ mV. The scale bars refer to all panels. **D**, Calcium channel current density–voltage relationship for control (□; $n = 36$), $\alpha_2\delta$ -1 HA (●; $n = 32$) and $\alpha_2\delta$ -1 MIDAS^{AAA} HA (▲; $n = 16$). In each experiment, current density (pA/pF) recorded in wild-type and mutant $\alpha_2\delta$ -1 HA overexpressing DRGs was normalized with respect to the control condition. At $+10$ and $+15$ mV, the current density of $\alpha_2\delta$ -1 HA overexpressing DRGs was significantly higher than the control condition ($p = 0.02$ one-way ANOVA and Dunnett’s test, $*p < 0.05$). **E**, Example of high K^+ -evoked Ca^{2+} transients in control neurons (left), wild-type $\alpha_2\delta$ -1 HA (middle), and $\alpha_2\delta$ -1 MIDAS^{AAA} HA (right) overexpressing DRG neurons. **F**, $\alpha_2\delta$ -1 HA neurons (gray bar; $n = 15$) showed a prolonged response duration with respect to $\alpha_2\delta$ -1 MIDAS^{AAA} HA (checked bar; $n = 15$) and control (open bar; $n = 15$) DRGs ($p = 0.006$ one-way ANOVA and Bonferroni *post hoc* test; $*p < 0.05$, $**p < 0.01$).

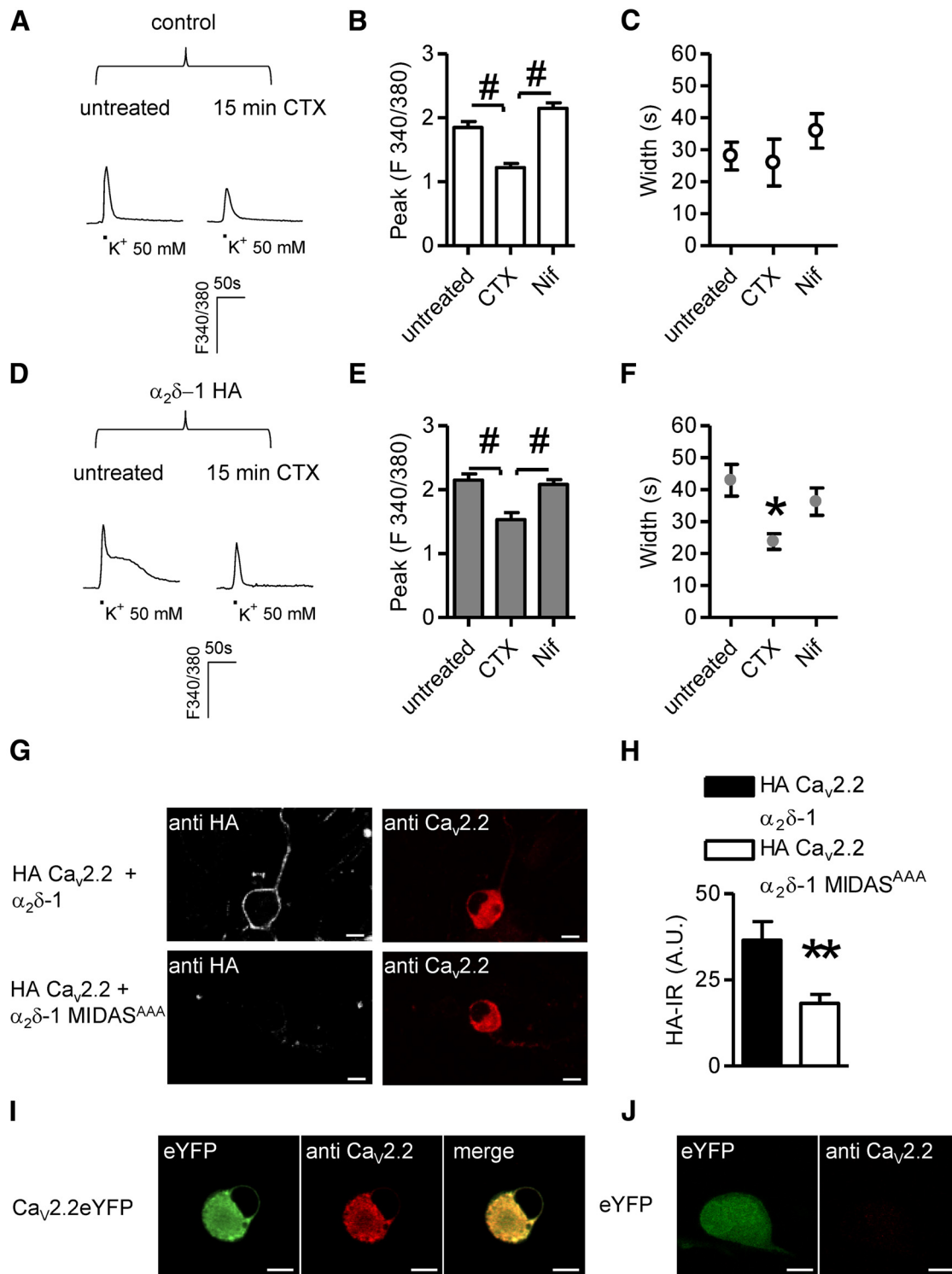


Figure 3. $Ca_v2.2$ -mediated signaling in $\alpha_2\delta$ -1 neurons. **A**, Imaging of high K^+ -evoked Ca^{2+} transients in control DRG neurons pretreated for 15 min with $1 \mu M$ CTX. **B**, In control DRG neurons, in the absence of $\alpha_2\delta$ -1 HA overexpression CTX application ($n = 7$) decreased the peak amplitude of responses with respect to untreated ($n = 21$) and Nif ($1 \mu M$; $n = 13$) samples ($p < 0.0001$ one-way ANOVA and Bonferroni *post hoc* test, $\#p < 0.001$). **C**, Inhibition of N- and L-type channels did not alter the width of signals imaged in control neurons ($p = 0.4$, one-way ANOVA). **D**, Examples of Ca^{2+} responses evoked in $\alpha_2\delta$ -1 HA overexpressing neurons in the absence (left) or presence (right) of CTX. **E**, CTX pretreatment ($n = 12$) diminished the intensity of signals in $\alpha_2\delta$ -1 HA overexpressing DRG neurons compared with responses obtained in untreated ($n = 19$) or Nif-treated ($n = 19$) DRGs ($p = 0.0001$ one-way ANOVA and Bonferroni *post hoc* test, $\#p < 0.001$). **F**, Prolonged high K^+ -evoked Ca^{2+} transients were abolished following CTX pretreatment ($p = 0.02$ one-way ANOVA and Bonferroni *post hoc* test, $*p < 0.05$). **G**, Overexpression in DRG neurons of exofacially HA-tagged $Ca_v2.2$, $\beta 1B$ subunits and either $\alpha_2\delta$ -1 (top) or $\alpha_2\delta$ -1 MIDAS^{AAA} (bottom). Surface and intracellular detection of HA $Ca_v2.2$ proteins was performed by staining the HA epitope in nonpermeabilizing conditions and intracellular labeling with an anti $Ca_v2.2$ antibody, respectively. Scale bars, $10 \mu m$. **H**, Quantification of surface HA staining in HA $Ca_v2.2/\alpha_2\delta$ -1/ $\beta 1B$ (black bar; $n = 32$) or HA $Ca_v2.2/\alpha_2\delta$ -1 MIDAS^{AAA}/ $\beta 1B$ (white bar; $n = 36$) transfected neurons ($p = 0.02$, *t* test). **I**, Labeling of overexpressed channels by $Ca_v2.2$ polyclonal antibody. DRG neurons were transfected with $Ca_v2.2$ eYFP and $\beta 1B$ cDNAs. **J**, $Ca_v2.2$ antibody failed to identify native subunits in eYFP overexpressing neurons indicating that the amount of protein is a limiting factor in immunocytochemistry experiments.

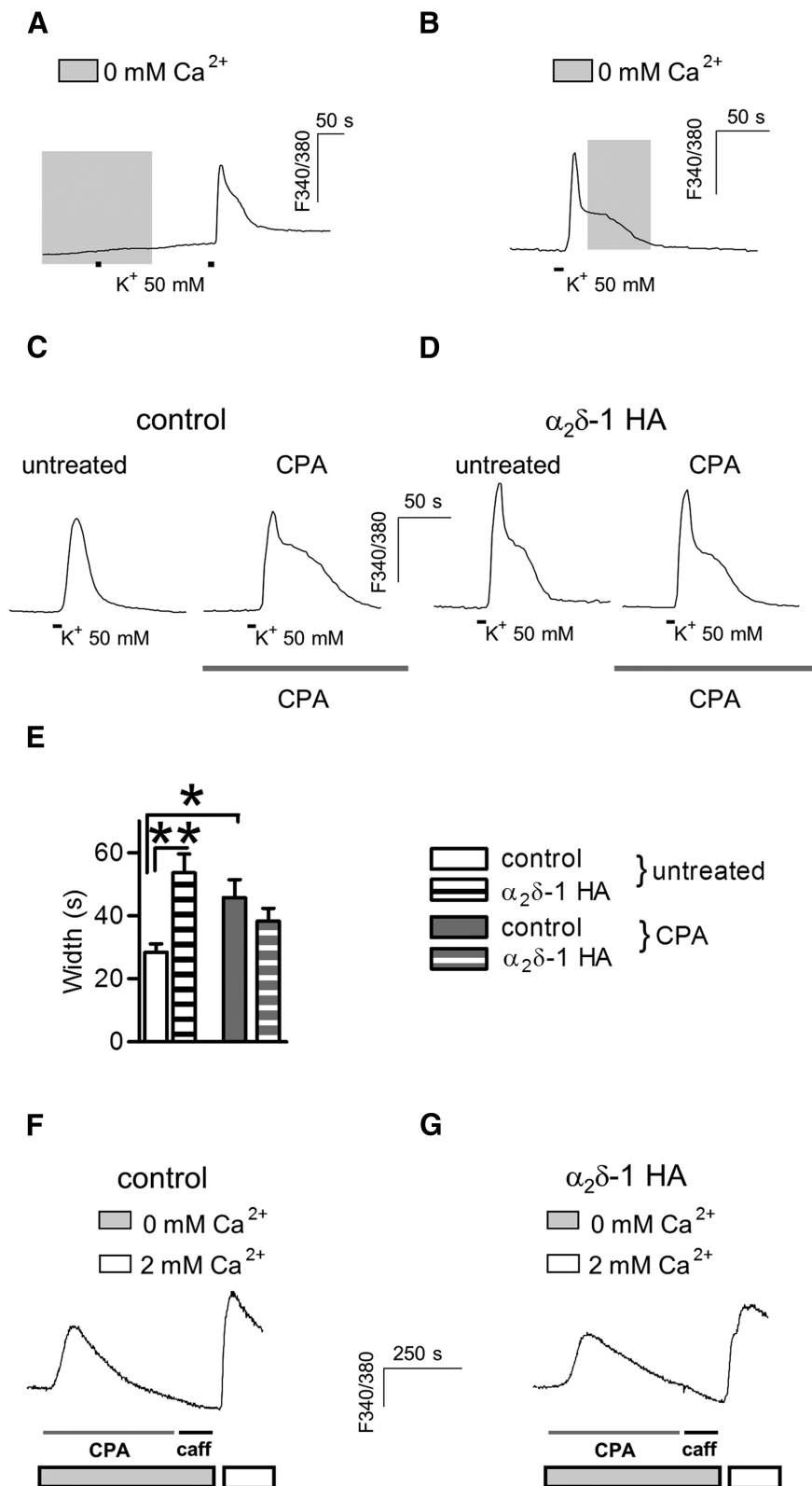


Figure 4. ER stores are not involved in shaping $\alpha_2\delta$ -1 HA prolonged responses. **A**, Preincubation of DRGs in Ca^{2+} free bathing solution during the period shown by the gray shading abolished high K^+ -induced transients. The response was recovered after a subsequent application of extracellular 2 mM Ca^{2+} . **B**, The Ca^{2+} hump observed in high K^+ -evoked signal of $\alpha_2\delta$ -1 HA overexpressing neurons is not affected by perfusion with 0 mM Ca^{2+} after the initiation of the peak response (representative of $n = 4$). **C, D**, High K^+ -evoked Ca^{2+} transients imaged before and after store depletion by CPA pretreatment (right trace; $5\ \mu\text{M}$, 15 min) in control (**C**) and $\alpha_2\delta$ -1 HA overexpressing neurons (**D**). **E**, Ca^{2+} transients evoked in $\alpha_2\delta$ -1 HA overexpressing DRGs (striped bars) were not altered by CPA preapplication (gray bars; $n = 14$) when compared with neurons processed in parallel without the drug (white bars; $n = 15$). By contrast, in control neurons, CPA pretreatment ($n = 14$) resulted in responses with a slower recovery

We compared the cell surface localization of HA-Cav2.2 when coexpressed with wild-type $\alpha_2\delta$ -1 or $\alpha_2\delta$ -1MIDAS^{AAA} (Fig. 3G). As shown in Figure 3G,H, surface expression of N-type channels was promoted by wild-type $\alpha_2\delta$ -1 relative to $\alpha_2\delta$ -1MIDAS^{AAA} (Fig. 3H). Total expression of N-type channels was assessed by staining permeabilized neurons with a Cav2.2 antibody directed against the intracellular II–III loop (Raghib et al., 2001). In immunocytochemistry experiments this antibody enabled detection of overexpressed Cav2.2 subunits only (Fig. 3I,J).

$\alpha_2\delta$ -1 HA modulation of Ca^{2+} transients is insensitive to depletion of the ER Ca^{2+} stores

What is the mechanism underlying the depolarization-evoked extended Ca^{2+} rise in $\alpha_2\delta$ -1 HA overexpressing neurons? Figure 4A shows that initiation of the high K^+ -induced response was dependent on extracellular Ca^{2+} , whereas the shape of the “hump” component did not change when $\alpha_2\delta$ -1 HA overexpressing DRGs were incubated in a Ca^{2+} -free bathing solution immediately after depolarization (Fig. 4B), indicating that the prolonged signal is mediated by Ca^{2+} release from intracellular compartments. The mechanism of calcium-induced calcium release from the ER has been found to regulate the depolarization-induced Ca^{2+} increase in a subpopulation of DRG neurons (Shmigol et al., 1995; Lu et al., 2006). To investigate the role of the ER in the $\alpha_2\delta$ -1-mediated response, we depleted intracellular stores with CPA, a selective blocker of the sarcoendoplasmic reticulum Ca^{2+} -ATPase (SERCA). Figure 4C,D shows example traces in untreated neurons, or after preincubation with CPA ($5\ \mu\text{M}$, 15 min), for both control (Fig. 4C) and $\alpha_2\delta$ -1 overexpressing cells (Fig. 4D). In the absence of $\alpha_2\delta$ -1 HA overexpression, CPA induced a widening of the response, implying a role for ER stores in Ca^{2+} clearance after depolarization. However, in $\alpha_2\delta$ -1 HA overexpressing neurons CPA did not affect the shape of Ca^{2+} transients (Fig. 4E). As expected, CPA application

←
than those from untreated neurons ($n = 14$; interaction: $p = 0.001$, two-way ANOVA and Bonferroni *post hoc* test, $*p < 0.05$, $**p < 0.01$). **F, G**, Application of CPA in Ca^{2+} -free solution (gray bar; $20\ \mu\text{M}$, 5 min). Caffeine (Caff; 5 mM) was then applied, and the lack of response indicated store depletion. Adding Ca^{2+} into the extracellular solution (white bar) triggered a similar store-operated calcium channel response in both control DRG neurons (**F**) and those overexpressing $\alpha_2\delta$ -1 HA (**G**).

increased baseline Ca^{2+} levels both in control (baseline before CPA: 0.98 ± 0.02 , $n = 15$; baseline after CPA: 1.11 ± 0.03 , $n = 15$; $p = 0.006$, paired t test) and in $\alpha_2\delta$ -1 HA overexpressing neurons (baseline before CPA: 0.92 ± 0.03 F340/380, $n = 14$; baseline after CPA: 1.15 ± 0.05 F340/380, $n = 14$; $p = 0.002$, paired t test), indicating a role for SERCA under resting conditions.

To investigate whether overexpression of $\alpha_2\delta$ -1 HA might interfere with the correct functioning of the ER stores, we applied CPA in a Ca^{2+} -free bathing solution and measured Ca^{2+} leak from the ER. Caffeine was then applied to assess the effectiveness of CPA-mediated store depletion. In addition we then monitored store-operated Ca^{2+} entry by reverting to 2 mM Ca^{2+} after store depletion (Fig. 4F,G). No difference in ER Ca^{2+} content was detected in $\alpha_2\delta$ -1 HA overexpressing DRGs (total area: 56.58 ± 7.36 , $n = 14$), compared with control neurons (total area: 51.24 ± 8.07 , $n = 13$; $p = 0.6$, t test). Furthermore upon CPA-mediated store depletion, the addition of extracellular Ca^{2+} to the bathing solution resulted in a store-operated Ca^{2+} channel response of equal peak amplitude between $\alpha_2\delta$ -1 overexpressing and control neurons (control: 0.83 ± 0.06 F340/380, $n = 11$; $\alpha_2\delta$ -1: 0.70 ± 0.04 , $n = 14$; $p = 0.1$, t test).

Mitochondria buffer signals enhanced by $\alpha_2\delta$ -1 HA upregulation

Mitochondria are important regulators of Ca^{2+} dynamics in DRG neuron cell bodies (Werth and Thayer, 1994) and neurite terminals (Medvedeva et al., 2008). These organelles accumulate Ca^{2+} into their matrix through a calcium uniporter mechanism driven by the negative mitochondrial membrane potential. Ca^{2+} is then slowly released back into the cytoplasm via $\text{Na}^+/\text{Ca}^{2+}$ exchangers (Rizzuto et al., 2012), and pumped out of the cell. We first used a pharmacological approach to identify the contribution of mitochondria to the Ca^{2+} response in $\alpha_2\delta$ -1 HA overexpressing DRGs. Figure 5 shows representative Ca^{2+} signals and quantification in control (Fig. 5A,B) and $\alpha_2\delta$ -1 HA overexpressing neurons (Fig. 5C,D) with or without the application of antimycin (anti; 0.3 μM) and oligomycin (oligo; 1 μM). The combination of these drugs has been previously found to be effective in blocking Ca^{2+} uptake into mitochondria while preventing ATP depletion (Medvedeva et al., 2008). When Ca^{2+} transients were evoked in the presence of antimycin and oligomycin, there was an increase in the peak amplitude of responses from both control (Fig. 5B) and $\alpha_2\delta$ -1 HA overexpress-

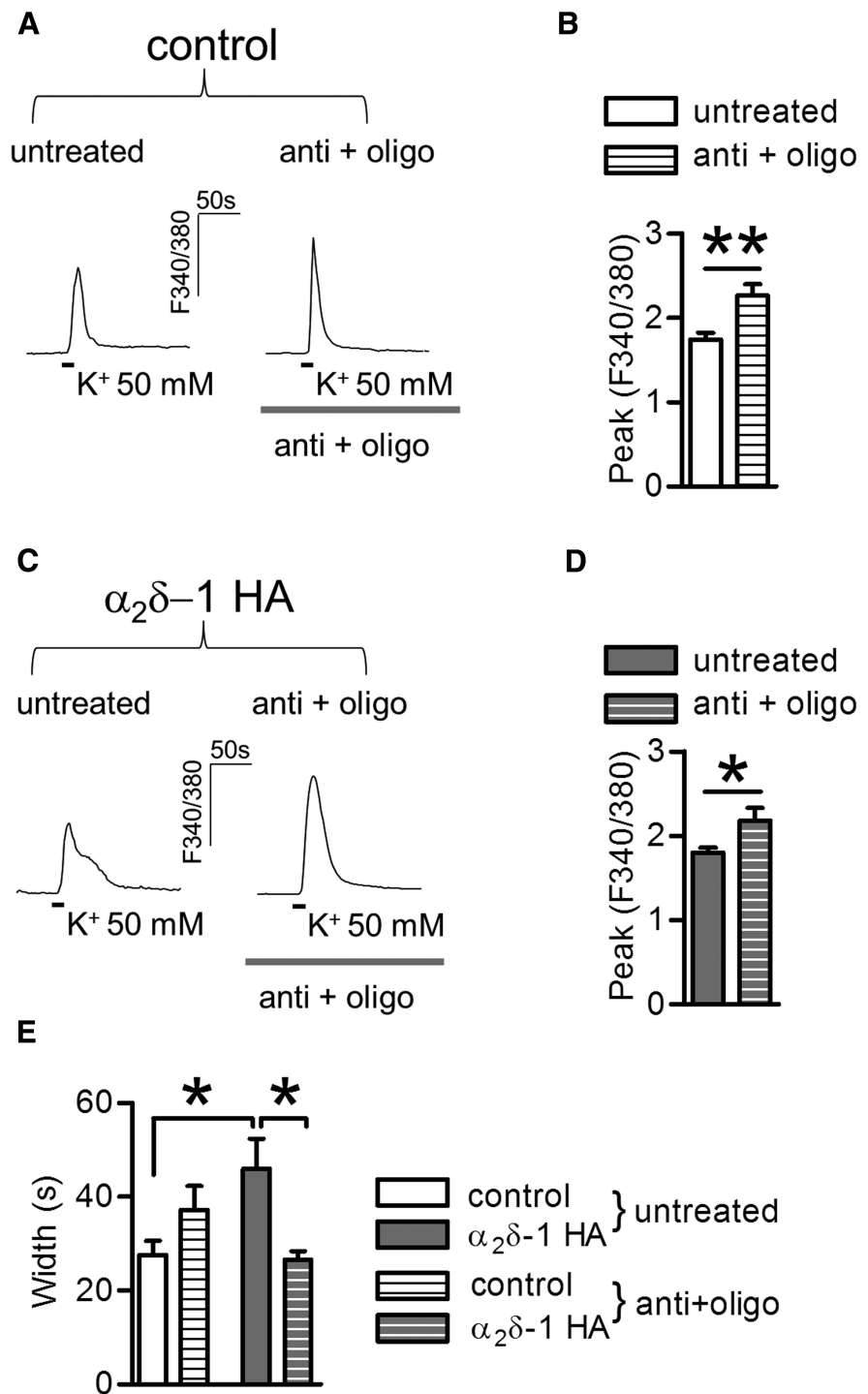


Figure 5. Role of mitochondria in the intracellular Ca^{2+} response in control and $\alpha_2\delta$ -1 HA overexpressing DRGs. **A**, High K^+ -triggered Ca^{2+} signals in the absence (left) or presence (right) of antimycin and oligomycin (anti + oligo; 5 min preapplication) in control DRG neurons. **B**, Quantification of peak response after the application of anti + oligo in control DRG neurons (striped bar; $n = 22$) compared with untreated neurons (open bar; $n = 19$) processed in parallel. The peak amplitude of responses is increased by anti + oligo application (** $p = 0.002$, t test). **C**, Example of Ca^{2+} transients imaged in $\alpha_2\delta$ -1 HA overexpressing DRGs following anti + oligo pretreatment, as in **A**. **D**, Quantification of peak response after the application of anti + oligo in $\alpha_2\delta$ -1 HA overexpressing DRG neurons (gray striped bar; $n = 20$) compared with untreated neurons processed in parallel (gray bar; $n = 27$; $*p = 0.03$, t test). **E**, The increased Ca^{2+} transient duration mediated by $\alpha_2\delta$ -1 HA overexpression (gray bars) compared with control DRG neurons (open bars) is inhibited by anti + oligo treatment (striped bars; two-way ANOVA and Bonferroni *post hoc* test, $*p < 0.05$).

ing DRGs (Fig. 5D). However, in the latter condition the hump component was abolished giving rise to a marked reduction of response duration (Fig. 5C,E). A significant interaction (Fig. 5E; $p = 0.004$, two-way ANOVA) between the drug treatment and

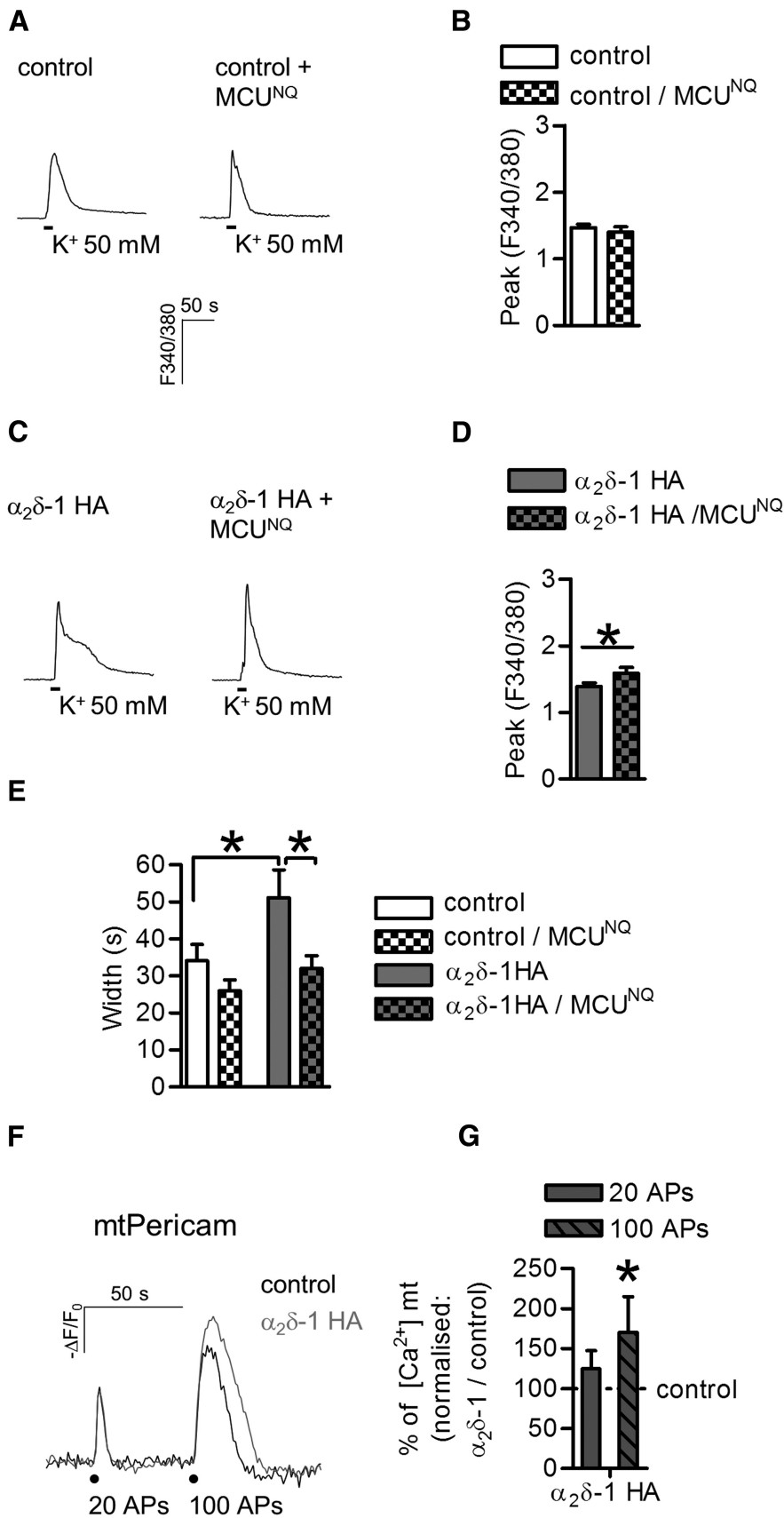


Figure 6. MCU contributes to generate the Ca^{2+} hump in DRGs overexpressing $\alpha_2\delta$ -1 HA. **A**, High K^+ -induced Ca^{2+} transients in control DRG neurons, in the absence (left; $n = 31$) or presence (right; $n = 22$) of MCU^{D260N,E263Q}. **B**, No change in the peak amplitude after MCU^{D260N,E263Q} overexpression (checked bar compared with open bar) in control DRG neurons ($p = 0.4$, t test). **C**, High K^+ -induced Ca^{2+} transients in $\alpha_2\delta$ -1 HA overexpressing (left; $n = 28$) and $\alpha_2\delta$ -1 HA + MCU^{D260N,E263Q} overexpressing

$\alpha_2\delta$ -1 overexpression underlined a synergistic action of the two factors.

The recent identification of the channel responsible for mitochondrial Ca^{2+} uptake (MCU) has allowed the development of more sensitive tools to study Ca^{2+} entry into mitochondria (De Stefani et al., 2011). Because the uniporter machinery involves the formation of a tetramer, we were able to use a dominant-negative form of MCU protein (MCU^{D260N,E263Q}; Raffaello et al., 2013) to knockdown mitochondrial calcium buffering in DRGs. As described previously (Raffaello et al., 2013), the overexpression of MCU^{D260N,E263Q} carrying two point mutations in the pore-forming domain oligomerize with endogenous subunits giving rise to a substantial reduction of calcium uptake into mitochondria ($\sim 47\%$ decrease of $[Ca^{2+}]_{mt}$). Calcium imaging experiments shown in Figure 6A indicate that in the absence of overexpressed $\alpha_2\delta$ -1 HA subunit the overexpression of MCU^{D260N,E263Q} (MCU^{NQ}) did not affect the amplitude of high K^+ -evoked Ca^{2+} transients (Fig. 6B). The discrepancy between this result and the data obtained with antimycin and oligomycin treatment is likely to be due to only a partial loss of function induced by MCU^{D260N,E263Q}, as many mitochondria retained functioning MCU machinery (Raffaello et al., 2013). Nevertheless when MCU^{D260N,E263Q} was cotransfected together with $\alpha_2\delta$ -1, the peak response showed a consistent increase of $21 \pm 9\%$ (Fig. 6C,D; $p = 0.04$). In addition the overexpression of MCU^{D260N,E263Q} exerted an effect on Ca^{2+} transient duration (Fig. 6E), leading to an inhibition of the prolonged Ca^{2+} rise in $\alpha_2\delta$ -1 HA overexpressing neurons, whereas no significant change was detected in the shape of signals in control DRGs. These findings showed

(right; $n = 23$) DRGs. **D**, Cotransfection of MCU^{D260N,E263Q} and $\alpha_2\delta$ -1 HA subunit increased the peak amplitude of high K^+ -induced Ca^{2+} transients (gray checked bar compared with solid gray bar, $*p < 0.05$, t test). **E**, Following MCU^{D260N,E263Q} overexpression, $\alpha_2\delta$ -1 HA neurons did not display prolonged Ca^{2+} response in response to 50 mM K^+ (gray checked bar compared with solid gray bar; $p = 0.01$ two-way ANOVA and Bonferroni *post hoc* test, $*p < 0.05$). There was no effect of MCU^{D260N,E263Q} on the response width in control DRG neurons (checked bar compared with open bar). **F**, MtPericam responses stimulated by the application of 20 and 100 APs at 10 Hz in control ($n = 26$; black trace) and $\alpha_2\delta$ -1 HA neurons ($n = 31$; top gray trace). **G**, Increase of 100 AP-induced mitochondrial Ca^{2+} uptake in the presence of $\alpha_2\delta$ -1 HA and normalized to $[Ca^{2+}]_{mt}$ in control neurons ($p = 0.034$; Kruskal–Wallis one-way ANOVA and Dunn’s multiple-comparison test, $*p < 0.05$).

that in the presence of $\alpha_2\delta$ -1 HA, increases in intracellular Ca^{2+} were rapidly taken up by mitochondria, and subsequently released into the cytoplasm resulting in a prolonged Ca^{2+} response.

To directly monitor changes in mitochondrial Ca^{2+} uptake following membrane depolarization, control and $\alpha_2\delta$ -1 HA overexpressing neurons were cotransfected with mtPericam (Nagai et al., 2001), a Ca^{2+} probe selectively localized within mitochondria. Stimulation of DRGs with 20 and 100 action potentials (APs) at 10 Hz induced a large increase in $[\text{Ca}^{2+}]_{\text{mt}}$ (Fig. 6F), confirming the role of mitochondria in buffering depolarization-evoked Ca^{2+} signals (Colegrove et al., 2000). Moreover, comparison between control and $\alpha_2\delta$ -1 HA overexpressing neurons demonstrated an augmented mitochondrial Ca^{2+} uptake in $\alpha_2\delta$ -1 HA overexpressing DRGs stimulated with 100 APs (Fig. 6G).

Because the rate of mitochondrial Ca^{2+} buffering correlates with changes in cytosolic Ca^{2+} levels (Colegrove et al., 2000), we increased Ca^{2+} entry by the application of 100 mM K^+ (experimental protocol shown in Fig. 7A) and assessed the contribution of $\text{MCU}^{\text{D260N,E263Q}}$ overexpression to Ca^{2+} transients evoked in control and $\alpha_2\delta$ -1 HA DRGs. This stronger depolarization protocol induced larger signals with a longer duration in both $\alpha_2\delta$ -1 HA overexpressing and control neurons (Fig. 7B), resulting in the generation of an equal duration of Ca^{2+} response in both conditions. As expected the inhibition of prolonged Ca^{2+} transients linked with $\text{MCU}^{\text{D260N,E263Q}}$ overexpression was strongly enhanced by 100 mM K^+ application (Fig. 7C). However only when $\text{MCU}^{\text{D260N,E263Q}}$ was coexpressed with $\alpha_2\delta$ -1 HA, was the shortening of the response width associated with a significant rise of the peak amplitude (~20% increase of F340/380 in $\alpha_2\delta$ -1 HA/MCU^{D260N,E263Q} vs ~5% increase in control/MCU^{D260N,E263Q}; Fig. 7D). This finding indicates that the activation of mitochondrial Ca^{2+} uptake depends, not only on the intensity of the response but also may be linked to a specific cellular pathway. Thus the upregulation of $\text{Ca}_v2.2$ channels in $\alpha_2\delta$ -1 HA overexpressing neurons may recruit mitochondria into a predominant role of shaping Ca^{2+} transients (Fig. 7E).

Activity-dependent reduction of mitochondrial trafficking in $\alpha_2\delta$ -1 HA overexpressing neurites

Mitochondria are dynamic organelles synthesized in the cell body and trafficked along neuronal processes at velocities ranging from 0.3 to 1 $\mu\text{m/s}$ (MacAskill and Kittler, 2010). They are char-

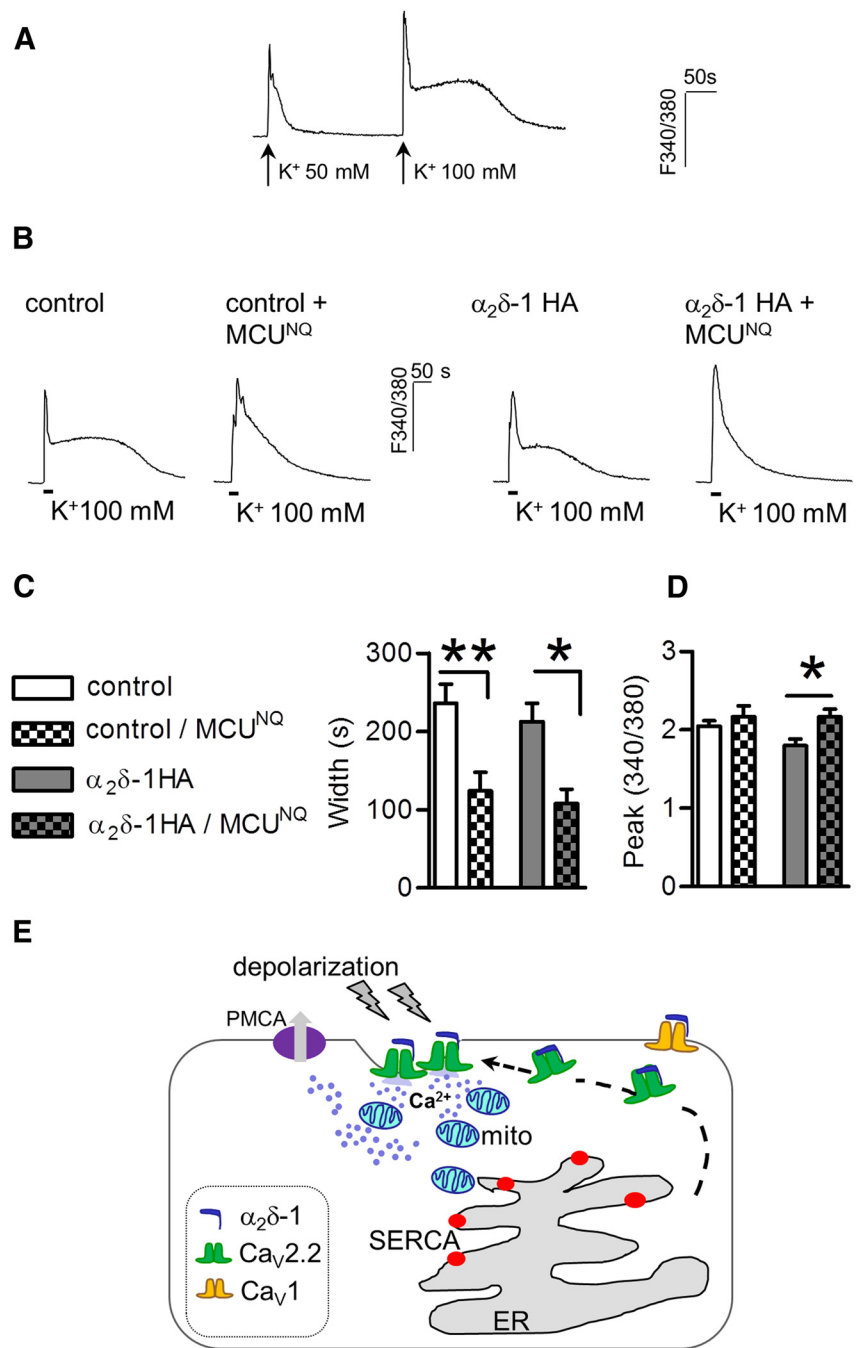


Figure 7. $\text{MCU}^{\text{D260N,E263Q}}$ effect on 100 mM K^+ -evoked Ca^{2+} response in control and $\alpha_2\delta$ -1 neurons. **A**, Increasing concentrations of KCl (50, 100 mM) correspond to a consequent elevation of peak and duration of Ca^{2+} transients imaged in control (representative of $n = 22$; $p < 0.0001$, paired t test) and $\alpha_2\delta$ -1 neurons ($n = 10$; $p < 0.0001$, $p < 0.0008$ for area and duration respectively, paired t test). **B**, Ca^{2+} traces triggered by the application of 100 mM K^+ (10 s) in control and $\alpha_2\delta$ -1 HA DRGs with or without the expression of MCU dominant negative. **C**, $\text{MCU}^{\text{D260N,E263Q}}$ overexpression significantly reduced duration of Ca^{2+} transients activated by 100 mM K^+ ($p = 0.0002$, two-way ANOVA and Bonferroni *post hoc* test, $*p < 0.05$, $**p < 0.01$). **D**, Quantification of peak amplitude of response in control ($n = 20$), control + $\text{MCU}^{\text{D260N,E263Q}}$ ($n = 13$), $\alpha_2\delta$ -1 HA ($n = 10$), and $\alpha_2\delta$ -1 HA + $\text{MCU}^{\text{D260N,E263Q}}$ ($n = 14$) DRGs. Overexpression of mutant MCU increased peak amplitude of signals imaged in $\alpha_2\delta$ -1 HA neurons only ($p = 0.02$, two-way ANOVA and Bonferroni *post hoc* test). **E**, Proposed mechanism for $\alpha_2\delta$ -1 regulation of activity dependent- Ca^{2+} signals. Increased levels of $\alpha_2\delta$ -1 protein lead to surface $\text{Ca}_v2.2$ channel upregulation. N-type channel-mediated Ca^{2+} influx is primarily buffered by mitochondria which contribute together with plasma membrane Ca^{2+} -ATPase (PMCA) to limit the amount of Ca^{2+} increase in the cytoplasm.

acterized by a bidirectional saltatory movement, which is regulated by intracellular Ca^{2+} levels (Wang and Schwarz, 2009). An increase in Ca^{2+} concentration induces the arrest of mitochondrial trafficking, leading to a rapid distribution of mitochondria in regions demanding high Ca^{2+} buffering. We hypothesized

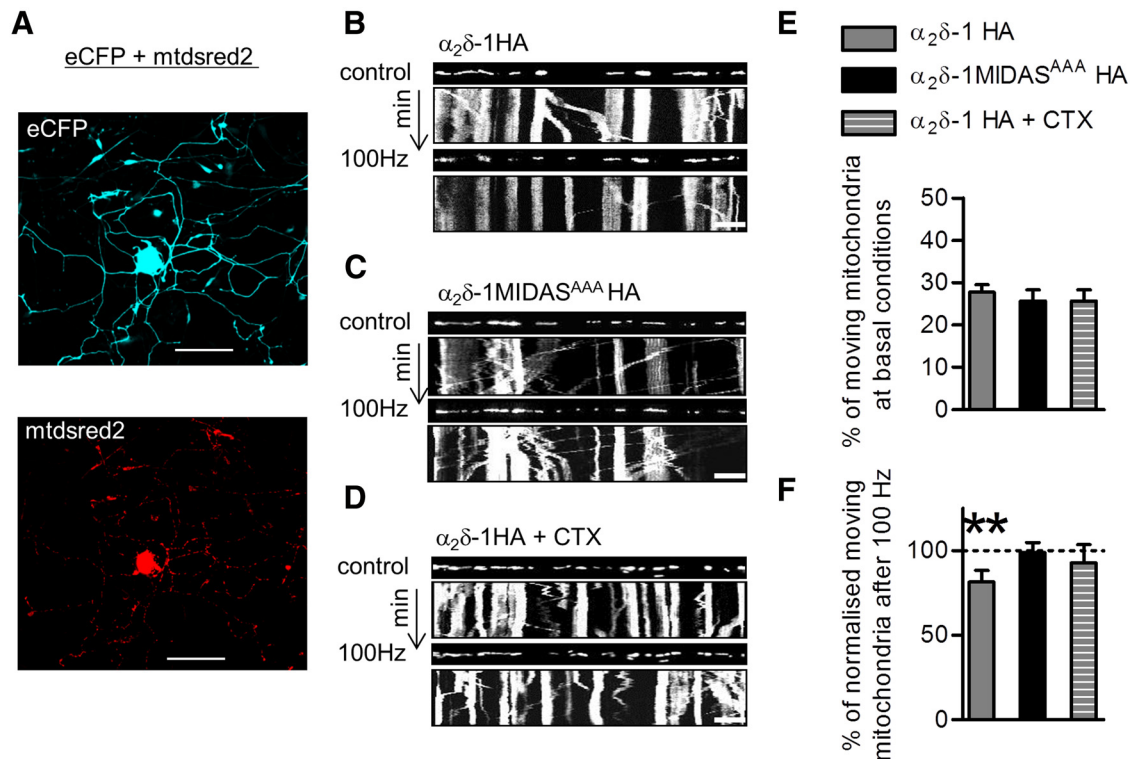


Figure 8. Reduction of axonal mitochondrial transport following electrical stimulation of $\alpha_2\delta$ -1 HA overexpressing DRG neurons. **A**, For time-lapse experiments, neurons were transfected with $\alpha_2\delta$ -1 HA and eCFP to identify neuron morphology (top image) together with pdsRed2-Mito plasmid to label mitochondria (bottom image). Scale bar, 100 μm . **B–D**, Kymographs showing mitochondrial motility before and during the application of field stimulation in $\alpha_2\delta$ -1 HA (**B**), $\alpha_2\delta$ -1 MIDAS^{AAA} HA (**C**), or $\alpha_2\delta$ -1 HA neurons pretreated with CTX (1 μM for 15 min; **D**). The first frame of the time-lapse movie is shown above each kymograph. Vertical arrows indicate a 2 min imaging period. Scale bars, 10 μm . **E**, No difference in the percentage of moving mitochondria between $\alpha_2\delta$ -1 HA-expressing DRGs (gray bar; $n = 239$ mitochondria), $\alpha_2\delta$ -1 MIDAS^{AAA} HA-expressing DRGs (black bar; $n = 219$ mitochondria), or $\alpha_2\delta$ -1-expressing DRGs treated with CTX (gray striped bar; $n = 234$ mitochondria) before field stimulation ($p = 0.7$, Kruskal–Wallis one-way ANOVA). **F**, The proportion of moving mitochondria after field stimulation was normalized with respect to the moving mitochondria in each resting condition, and was decreased in $\alpha_2\delta$ -1 HA-expressing DRGs (gray bar; $p = 0.01$, Kruskal–Wallis one-way ANOVA and Dunn’s multiple-comparison test, $**p < 0.01$).

that by promoting VGCC trafficking, $\alpha_2\delta$ -1 HA overexpression might increase local Ca^{2+} influx within the neurites and exert an effect on mitochondrial axonal transport. We measured mitochondrial motility in wild-type and $\alpha_2\delta$ -1 MIDAS^{AAA} overexpressing DRGs, both in resting conditions and during field stimulation at 100 Hz. Mtdsred2 (Macaskill et al., 2009), a fluorescent protein exclusively localized in mitochondria (Fig. 8A, bottom), was used to visualize these organelles in the neurites during time lapse imaging experiments. Kymographs were generated to identify mobile and stationary mitochondria (Fig. 8B–D). The overexpression of $\alpha_2\delta$ -1 HA or $\alpha_2\delta$ -1 MIDAS^{AAA} mutant did not change the percentage of moving mitochondria in resting conditions (Fig. 8E). By contrast, intense electrical stimulation significantly reduced the fraction of moving mitochondria in $\alpha_2\delta$ -1 HA-expressing neurons compared with nonstimulated conditions (Fig. 8F). In-line with the finding that calcium channel abundance at presynaptic sites is controlled by the level of expression of wild-type $\alpha_2\delta$ -1 subunit (Hoppa et al., 2012), in the presence of $\alpha_2\delta$ -1 MIDAS^{AAA} HA we found no difference in the percentage of moving mitochondria before and after stimulation. Furthermore after $\alpha_2\delta$ -1 HA overexpressing cultures were pretreated with CTX (1 μM , 15 min; Fig. 8D), field stimulation did not cause mitochondria to stall, suggesting that the increased Ca^{2+} influx in response to depolarization is mainly mediated by $\text{Ca}_v2.2$ channels trafficked to the neurites by the $\alpha_2\delta$ -1 subunit.

Discussion

VGCC $\alpha_2\delta$ subunits are key molecules in the regulation of sensory neuron plasticity as their upregulation *per se* exerts effects on nociceptive behavior (Li et al., 2006). Moreover increased $\alpha_2\delta$ -1 protein levels in damaged DRG neurons contribute to the enhanced neurotransmission and hyperexcitability observed in neuropathic pain models (Campbell and Meyer, 2006; Patel et al., 2013), although no details about the molecular mechanisms have been reported.

In this work, we describe an *in vitro* model to study cellular changes triggered by increased $\alpha_2\delta$ -1 protein levels. Our data show that $\alpha_2\delta$ -1 HA upregulation enhances Ca^{2+} signal duration in response to brief membrane depolarization. Ca^{2+} transients were characterized by an initial peak followed by a prolonged Ca^{2+} rise, which did not depend on extracellular calcium. Similar effects on evoked Ca^{2+} responses have been observed *in vivo* in DRGs subjected to inflammatory insult (Fuchs et al., 2007; Lu and Gold, 2008). Surprisingly, in our assays the generation of this Ca^{2+} hump was mainly associated with N-type calcium channel activity as it was blocked by CTX, but not by application of the L-type channel blocker nifedipine. Also $\alpha_2\delta$ -1 HA overexpression prolonged the duration of Ca^{2+} transients evoked by field stimulation at 100 Hz frequency but did not change the shape of 10 Hz-triggered responses. This result is in agreement with the finding that 100 Hz-evoked Ca^{2+} signals are preferentially mediated by Ca_v2 channels (Wheeler et al., 2012). The experiments performed with mtPericam, confirmed this phenomenon, indicat-

ing a prominent role of mitochondria in buffering intracellular Ca^{2+} in response to a strong depolarization in $\alpha_2\delta$ -1 overexpressing neurons, compared with the control condition.

Functional data related to the effect of the $\alpha_2\delta$ -1 HA subunit on the intracellular Ca^{2+} rise through a CTX-sensitive pathway were confirmed by the increased surface detection of transfected $\text{Ca}_v2.2$ channels in $\alpha_2\delta$ -1 overexpressing cultures.

The ability of the $\alpha_2\delta$ -1 subunit to promote calcium channel expression at the cell surface is dependent on the MIDAS motif located in the VWA domain of $\alpha_2\delta$ proteins, as also shown in a neuronal cell line (Cassidy et al., 2014). Mutation of this motif markedly decreased $\alpha_2\delta$ -1 HA membrane expression, leading to a consequent reduction of $\text{Ca}_v2.2$ surface localization and complete inhibition of the prolonged Ca^{2+} response. Furthermore, the experiments performed with $\alpha_2\delta$ -1 MIDAS^{AAA} HA showed that the modulation of Ca^{2+} responses is dependent on the control of VGCC trafficking by $\alpha_2\delta$ -1, yet it provokes the question of the mechanism responsible for prolonged N-type VGCC-mediated Ca^{2+} transients.

Recently it has been postulated that intracellular Ca^{2+} signals triggered by different means can follow individual pathways coupled to specific cellular responses, such as the activation of gene transcription by Ca_v1 channels in sympathetic neurons (Wheeler et al., 2012). In the same neuronal model, using a $\text{Ca}_v2.1$ antibody, these VGCCs were found to be distributed in high-density patches in close proximity to ER–mitochondria interaction sites and it was postulated that Ca_v2 -mediated Ca^{2+} influx was preferentially sequestered by mitochondria. ER stores and mitochondria constitute the main Ca^{2+} buffering compartments in DRG neurons (Medvedeva et al., 2008). In our study, the inhibition of SERCA in control neurons slowed the recovery from high- K^+ evoked responses. This confirmed the role of the ER in Ca^{2+} clearance after depolarization. However, upon $\alpha_2\delta$ -1 overexpression, ER stores failed to further prolong depolarization-induced Ca^{2+} signals, despite contributing to resting Ca^{2+} levels, suggesting that the ER stores are full in this condition.

To investigate the role of mitochondria in the modulation of Ca^{2+} signaling by $\alpha_2\delta$ -1, we selectively knocked down the mitochondrial Ca^{2+} uniporter mechanism through the expression of a mutated MCU protein, $\text{MCU}^{\text{D260N,E263Q}}$. Cotransfection of $\text{MCU}^{\text{D260N,E263Q}}$ together with the $\alpha_2\delta$ -1 HA subunit in DRGs abolished the elevation of the Ca^{2+} transient width and increased response peak amplitude, when compared with neurons overexpressing $\alpha_2\delta$ -1 HA protein alone. Similar results were obtained when mitochondrial Ca^{2+} uptake was indirectly blocked by acute disruption of the mitochondrial membrane potential with antimycin and oligomycin treatment. Also with mtPericam imaging we were able to directly measure the increase in $[\text{Ca}^{2+}]_{\text{mt}}$ evoked by 100 AP stimulation of $\alpha_2\delta$ -1 HA-expressing neurons.

Altogether our genetic and pharmacological studies confirm that the activation of mitochondrial Ca^{2+} uptake is an essential mechanism called into play to limit the Ca^{2+} rise in response to Ca^{2+} entry (Friel, 2000), and define the $\alpha_2\delta$ -1 protein as a crucial regulator of VGCC-mediated signaling in peripheral neurons. Because mitochondria are recruited to buffer high Ca^{2+} loads (Werth and Thayer, 1994), it is likely that their involvement in $\alpha_2\delta$ -1-modulated signaling may be associated with an increase in the magnitude of Ca^{2+} response consequent on VGCC upregulation. Indeed, we found that stimulation of cultures with 100 mM K^+ increased the duration of Ca^{2+} responses, as well as the peak amplitude. In this condition, we found that almost all responses in both $\alpha_2\delta$ -1 HA overexpressing and control neurons were char-

acterized by a large plateau phase, which followed the initial rise of the peak. However the inhibition of mitochondrial Ca^{2+} uptake by $\text{MCU}^{\text{D260N,E263Q}}$ overexpression revealed that mitochondria contributed to blunting the Ca^{2+} response amplitude only in $\alpha_2\delta$ -1 overexpressing DRGs, suggesting that even in the presence of high Ca^{2+} entry, $\alpha_2\delta$ -1 HA overexpression displays a role in promoting mitochondrial Ca^{2+} buffering of N-type calcium channel-mediated responses, suggesting that they may be in proximity.

On the basis of data related to surface staining of $\text{Ca}_v2.2$ channels and lack of effect of the SERCA pump blocker in $\alpha_2\delta$ -1 HA overexpressing DRGs, we can speculate that mitochondria may preferentially buffer Ca^{2+} in close proximity to the channels at the plasma membrane. Conversely, in the absence of the $\alpha_2\delta$ -1 modulation of VGCC, mitochondria are more likely to be influenced by Ca^{2+} release from the ER. Previously it has been shown that mitochondria play an important role in the control of neurotransmission at presynaptic terminals both in capsaicin-sensitive DRGs and at central synapses (Billups and Forsythe, 2002; Medvedeva et al., 2008; Perkins et al., 2010). To regulate metabolic demand and the local intracellular Ca^{2+} concentration, mitochondria are rapidly trafficked through neuronal processes (Sheng and Cai, 2012). In agreement with the finding that mitochondrial stalling is Ca^{2+} -dependent in neuronal processes (Macaskill et al., 2009), we found that mitochondrial axonal transport was selectively reduced after electrical stimulation of $\alpha_2\delta$ -1 HA overexpressing cultures. In contrast, no change was observed in mitochondrial trafficking either in $\alpha_2\delta$ -1 MIDAS^{AAA} HA-expressing DRGs or in CTX-treated $\alpha_2\delta$ -1 HA overexpressing neurons. Our findings suggest that $\alpha_2\delta$ -1 HA overexpression may contribute to the formation of domains predominantly buffered by mitochondria in the cell body, as well as the axons of DRGs.

In conclusion, this work describes the mechanism through which $\alpha_2\delta$ -1 upregulation modulates the response of DRG neurons to depolarization, suggesting that N-type VGCC-mediated activation of mitochondrial Ca^{2+} buffering may contribute to intracellular signaling related to the aberrant neurotransmission in pathological conditions.

References

- Akimzhanov AM, Boehning D (2011) Monitoring dynamic changes in mitochondrial calcium levels during apoptosis using a genetically encoded calcium sensor. *J Vis Exp* 50:2579. [CrossRef Medline](#)
- Basbaum AI, Bautista DM, Scherrer G, Julius D (2009) Cellular and molecular mechanisms of pain. *Cell* 139:267–284. [CrossRef Medline](#)
- Bauer CS, Nieto-Rostro M, Rahman W, Tran-Van-Minh A, Ferron L, Douglas L, Kadurin I, Sri Ranjan Y, Fernandez-Alacid L, Millar NS, Dickenson AH, Lujan R, Dolphin AC (2009) The increased trafficking of the calcium channel subunit $\alpha_2\delta$ -1 to presynaptic terminals in neuropathic pain is inhibited by the $\alpha_2\delta$ ligand pregabalin. *J Neurosci* 29:4076–4088. [CrossRef Medline](#)
- Bauer CS, Tran-Van-Minh A, Kadurin I, Dolphin AC (2010) A new look at calcium channel $\alpha_2\delta$ subunits. *Curr Opin Neurobiol* 20:563–571. [CrossRef Medline](#)
- Bell TJ, Thaler C, Castiglioni AJ, Helton TD, Lipscombe D (2004) Cell-specific alternative splicing increases calcium channel current density in the pain pathway. *Neuron* 41:127–138. [CrossRef Medline](#)
- Berridge MJ (1998) Neuronal calcium signaling. *Neuron* 21:13–26. [CrossRef Medline](#)
- Berridge MJ, Bootman MD, Roderick HL (2003) Calcium signalling: dynamics, homeostasis and remodelling. *Nat Rev Mol Cell Biol* 4:517–529. [CrossRef Medline](#)
- Billups B, Forsythe ID (2002) Presynaptic mitochondrial calcium sequestration influences transmission at mammalian central synapses. *J Neurosci* 22:5840–5847. [Medline](#)

- Campbell JN, Meyer RA (2006) Mechanisms of neuropathic pain. *Neuron* 52:77–92. [CrossRef Medline](#)
- Canti C, Nieto-Rostro M, Foucault I, Heblich F, Wratten J, Richards MW, Hendrich J, Douglas L, Page KM, Davies A, Dolphin AC (2005) The metal-ion-dependent adhesion site in the von Willebrand factor-A domain of $\alpha_2\delta$ subunits is key to trafficking voltage-gated Ca^{2+} channels. *Proc Natl Acad Sci U S A* 102:11230–11235. [CrossRef Medline](#)
- Cassidy JS, Ferron L, Kadurin I, Pratt WS, Dolphin AC (2014) Functional exofacially tagged N-type calcium channels elucidate the interaction with auxiliary $\alpha_2\delta$ -1 subunits. *Proc Natl Acad Sci U S A* 111:8979–8984. [CrossRef Medline](#)
- Colegrove SL, Albrecht MA, Friel DD (2000) Dissection of mitochondrial Ca^{2+} uptake and release fluxes in situ after depolarization-evoked $[\text{Ca}^{2+}]_i$ elevations in sympathetic neurons. *J Gen Physiol* 115:351–370. [CrossRef Medline](#)
- De Stefani D, Raffaello A, Teardo E, Szabò I, Rizzuto R (2011) A forty-kilodalton protein of the inner membrane is the mitochondrial calcium uniporter. *Nature* 476:336–340. [CrossRef Medline](#)
- Dolphin AC (2012) Calcium channel auxiliary $\alpha_2\delta$ and β subunits: trafficking and one step beyond. *Nat Rev Neurosci* 13:542–555. [CrossRef Medline](#)
- Fernyhough P, Calcutt NA (2010) Abnormal calcium homeostasis in peripheral neuropathies. *Cell Calcium* 47:130–139. [CrossRef Medline](#)
- Friel DD (2000) Mitochondria as regulators of stimulus-evoked calcium signals in neurons. *Cell Calcium* 28:307–316. [CrossRef Medline](#)
- Fuchs A, Rigaud M, Hogan QH (2007) Painful nerve injury shortens the intracellular Ca^{2+} signal in axotomized sensory neurons of rats. *Anesthesiology* 107:106–116. [CrossRef Medline](#)
- Hoppa MB, Lana B, Margas W, Dolphin AC, Ryan TA (2012) $\alpha_2\delta$ Expression sets presynaptic calcium channel abundance and release probability. *Nature* 486:122–125. [CrossRef Medline](#)
- Julius D, Basbaum AI (2001) Molecular mechanisms of nociception. *Nature* 413:203–210. [CrossRef Medline](#)
- Kadurin I, Alvarez-Laviada A, Ng SF, Walker-Gray R, D'Arco M, Fadel MG, Pratt WS, Dolphin AC (2012) Calcium currents are enhanced by $\alpha_2\delta$ -1 lacking its membrane anchor. *J Biol Chem* 287:33554–33566. [CrossRef Medline](#)
- Karra D, Dahm R (2010) Transfection techniques for neuronal cells. *J Neurosci* 30:6171–6177. [CrossRef Medline](#)
- Li CY, Zhang XL, Matthews EA, Li KW, Kurwa A, Boroujerdi A, Gross J, Gold MS, Dickenson AH, Feng G, Luo ZD (2006) Calcium channel $\alpha_2\delta_1$ subunit mediates spinal hyperexcitability in pain modulation. *Pain* 125:20–34. [CrossRef Medline](#)
- Lu SG, Gold MS (2008) Inflammation-induced increase in evoked calcium transients in subpopulations of rat dorsal root ganglion neurons. *Neuroscience* 153:279–288. [CrossRef Medline](#)
- Lu SG, Zhang X, Gold MS (2006) Intracellular calcium regulation among subpopulations of rat dorsal root ganglion neurons. *J Physiol* 577:169–190. [CrossRef Medline](#)
- MacAskill AF, Kittler JT (2010) Control of mitochondrial transport and localization in neurons. *Trends Cell Biol* 20:102–112. [CrossRef Medline](#)
- MacAskill AF, Rinholm JE, Twelvetrees AE, Arancibia-Carcamo IL, Muir J, Fransson A, Aspenstrom P, Attwell D, Kittler JT (2009) Miro1 is a calcium sensor for glutamate receptor-dependent localization of mitochondria at synapses. *Neuron* 61:541–555. [CrossRef Medline](#)
- Medvedeva YV, Kim MS, Usachev YM (2008) Mechanisms of prolonged presynaptic Ca^{2+} signaling and glutamate release induced by TRPV1 activation in rat sensory neurons. *J Neurosci* 28:5295–5311. [CrossRef Medline](#)
- Meijering E, Jacob M, Sarria JC, Steiner P, Hirling H, Unser M (2004) Design and validation of a tool for neurite tracing and analysis in fluorescent microscopy images. *Cytometry A* 58:167–176. [CrossRef Medline](#)
- Nagai T, Sawano A, Park ES, Miyawaki A (2001) Circularly permuted green fluorescent proteins engineered to sense Ca^{2+} . *Proc Natl Acad Sci U S A* 98:3197–3202. [CrossRef Medline](#)
- Page KM, Heblich F, Margas W, Pratt WS, Nieto-Rostro M, Chaggar K, Sandhu K, Davies A, Dolphin AC (2010) N terminus is key to the dominant negative suppression of $\text{Ca}(\text{V})_2$ calcium channels: implications for episodic ataxia type 2. *J Biol Chem* 285:835–844. [CrossRef Medline](#)
- Patel R, Bauer CS, Nieto-Rostro M, Margas W, Ferron L, Chaggar K, Crews K, Ramirez JD, Bennett DL, Schwartz A, Dickenson AH, Dolphin AC (2013) $\alpha_2\delta$ -1 Gene deletion affects somatosensory neuron function and delays mechanical hypersensitivity in response to peripheral nerve damage. *J Neurosci* 33:16412–16426. [CrossRef Medline](#)
- Perkins GA, Tjong J, Brown JM, Poquiz PH, Scott RT, Kolson DR, Ellisman MH, Spirou GA (2010) The micro-architecture of mitochondria at active zones: electron tomography reveals novel anchoring scaffolds and cristae structured for high-rate metabolism. *J Neurosci* 30:1015–1026. [CrossRef Medline](#)
- Raffaello A, De Stefani D, Sabbadin D, Teardo E, Merli G, Picard A, Checchetto V, Moro S, Szabò I, Rizzuto R (2013) The mitochondrial calcium uniporter is a multimer that can include a dominant-negative pore-forming subunit. *EMBO J* 32:2362–2376. [CrossRef Medline](#)
- Raghib A, Bertaso F, Davies A, Page KM, Meir A, Bogdanov Y, Dolphin AC (2001) Dominant-negative synthesis suppression of voltage-gated calcium channel $\text{Cav}2.2$ induced by truncated constructs. *J Neurosci* 21:8495–8504. [Medline](#)
- Rizzuto R, De Stefani D, Raffaello A, Mammucari C (2012) Mitochondria as sensors and regulators of calcium signalling. *Nat Rev Mol Cell Biol* 13:566–578. [CrossRef Medline](#)
- Scroggs RS, Fox AP (1992) Calcium current variation between acutely isolated adult rat dorsal root ganglion neurons of different size. *J Physiol* 445:639–658. [CrossRef Medline](#)
- Sheng ZH, Cai Q (2012) Mitochondrial transport in neurons: impact on synaptic homeostasis and neurodegeneration. *Nat Rev Neurosci* 13:77–93. [CrossRef Medline](#)
- Shmigol A, Verkhratsky A, Isenberg G (1995) Calcium-induced calcium release in rat sensory neurons. *J Physiol* 489:627–636. [CrossRef Medline](#)
- Shutov LP, Kim MS, Houlihan PR, Medvedeva YV, Usachev YM (2013) Mitochondria and plasma membrane Ca^{2+} -ATPase control presynaptic Ca^{2+} clearance in capsaicin-sensitive rat sensory neurons. *J Physiol* 591:2443–2462. [CrossRef Medline](#)
- Tinker A, Jan YN, Jan LY (1996) Regions responsible for the assembly of inwardly rectifying potassium channels. *Cell* 87:857–868. [CrossRef Medline](#)
- Usachev YM, Thayer SA (1997) All-or-none Ca^{2+} release from intracellular stores triggered by Ca^{2+} influx through voltage-gated Ca^{2+} channels in rat sensory neurons. *J Neurosci* 17:7404–7414. [Medline](#)
- Wang X, Schwarz TL (2009) The mechanism of Ca^{2+} -dependent regulation of kinesin-mediated mitochondrial motility. *Cell* 136:163–174. [CrossRef Medline](#)
- Werth JL, Thayer SA (1994) Mitochondria buffer physiological calcium loads in cultured rat dorsal root ganglion neurons. *J Neurosci* 14:348–356. [Medline](#)
- Wheeler DG, Groth RD, Ma H, Barrett CF, Owen SF, Safa P, Tsien RW (2012) $\text{Ca}(\text{V})_1$ and $\text{Ca}(\text{V})_2$ channels engage distinct modes of Ca^{2+} signaling to control CREB-dependent gene expression. *Cell* 149:1112–1124. [CrossRef Medline](#)
- Wood JN, Winter J, James IF, Rang HP, Yeats J, Bevan S (1988) Capsaicin-induced ion fluxes in dorsal root ganglion cells in culture. *J Neurosci* 8:3208–3220. [Medline](#)
- Xiao HS, Huang QH, Zhang FX, Bao L, Lu YJ, Guo C, Yang L, Huang WJ, Fu G, Xu SH, Cheng XP, Yan Q, Zhu ZD, Zhang X, Chen Z, Han ZG, Zhang X (2002) Identification of gene expression profile of dorsal root ganglion in the rat peripheral axotomy model of neuropathic pain. *Proc Natl Acad Sci U S A* 99:8360–8365. [CrossRef Medline](#)